Numerical calculation of axisymmetric nonneutral plasma equilibria

Ross L. Spencer, S. N. Rasband, and Richard R. Vanfleet

Numerical calculation of axisymmetric non-neutral plasma equilibria

Ross L. Spencer, S. N. Rasband, and Richard R. Vanfleet
Department of Physics and Astronomy, Brigham Young University, Provo, Utah 84602

Efficient techniques for computing axisymmetric non-neutral plasma equilibria are described. These equilibria may be obtained either by requiring global thermal equilibrium, by specifying the midplane radial density profile, or by specifying the radial profile of $\int n \, dz$. Both splines and finite-differences are used, and the accuracy of the two is compared by using a new characterization of the thermal equilibrium density profile which gives a simple formula for estimating the radial and axial gradient scale lengths of thermal equilibria. It is found that for global thermal equilibrium 1% accuracy is achieved with splines if the distance between neighboring splines is about two Debye lengths while finite differences require a grid spacing of about one-half Debye length to achieve the same accuracy.

I. INTRODUCTION

The equation which determines cylindrically symmetric non-neutral plasma equilibria of the kind studied by Malmberg and others[1,2] is simply Poisson's equation in the form

$$\nabla^2 \phi = -\frac{q}{\epsilon_0} n(r,z) = f(r,\phi) \qquad (1)$$

(see, for example, Ref. 2). In this equation ϕ is the electrostatic potential, q is the particle charge, n is the particle density, r is the radial coordinate, z is the axial coordinate, and ϵ_0 is the permittivity of free space. The right-hand side of this equation is generally a nonlinear function of ϕ, making it similar to the Grad–Shafranov equation in the study of magnetohydrodynamic equilibrium.[3] These problems have been solved for years by various iteration schemes, and two of these schemes have been found to be particularly simple and effective in the present problem: (i) Picard iteration with splines and underrelaxation, and (ii) simultaneous overrelaxation (SOR) with finite-differences and Newton's method (Newton SOR). These two methods as applied to Eq. (1) are the subject of this paper. We find that the finite-difference representation with Newton SOR is the simplest to use if only moderate accuracy is required. For high accuracy calculations, however, the spline representation is better because a good approximation to the solution is obtained with a relatively small number of splines, and the splines naturally provide a high-order interpolation method. Also, under conditions of comparable accuracy, spline equilibria run about 50% faster.

The cylindrical geometry for these computations is shown in Fig. 1, where both density and potential contours in the r-z plane are shown. The computation region has radius a and length b. As is usual in these systems we assume that the plasma is axisymmetric and that it is confined radially by a strong magnetic field parallel to the axis

of the cylinder and axially by voltages applied to conducting end rings. The boundary conditions on ϕ are

$$\frac{\partial \phi}{\partial r} = 0 \quad \text{at } r = 0; \qquad (2)$$

$$\frac{\partial \phi}{\partial z} = 0 \quad \text{at } z = 0; \qquad (3)$$

$$\phi = 0 \quad \text{at } z = b. \qquad (4)$$

Also, at the conducting wall $\phi = \phi(a,z)$ is zero except at the location of the confining ring. Note that these boundary conditions are appropriate for computing an axisymmetric half-equilibrium with reflection symmetry about $z = 0$, as shown in Fig. 1. Full equilibria can also be computed by the techniques described here. Finally, a special condition must be placed on the function $f(r,\phi)$ on the right-hand side of Eq. (1), namely, that it is zero beyond the confining rings. The exact way in which this condition is implemented is somewhat a matter of taste, but without it every algorithm we have tried converges to a state with plasma beyond the rings.

In this paper we discuss three different ways of obtaining equilibria, each corresponding to a different way of specifying the right-hand side of Eq. (1): (i) global thermal equilibrium,[2] (ii) choosing a midplane density profile, $n(r,z=0)$, and (iii) choosing a line density profile, $g(r) = \int_0^b n(r,z) dz$. These are discussed in Sec. II. We then discuss how to calculate these equilibria using splines and Picard iteration in Sec. III and how to calculate them with finite-differences using simultaneous overrelaxtion with Newton's method (Newton SOR) in Sec. IV. Finally, in Sec. V we test both calculation methods by comparing them with well-known properties of thermal equilibria[2,4,5] and with a new formula for the density gradient scale length. Section VI concludes the paper.
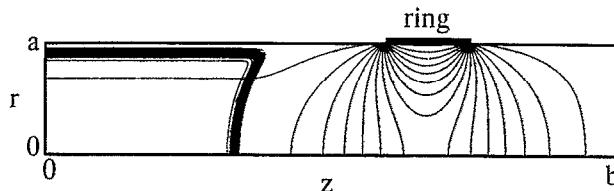
FIG. 1. Non-neutral plasma geometry with contours of constant potential and density both shown. The plasma is confined radially by a strong axial magnetic field and axially by potentials applied to end rings. For convenience, only one-quarter of the full geometry is shown here. The potential applied to the outer cylinder is zero, except at the confining rings. The cylinder radius is $a=0.04$ m, the length is $b=0.2$ m, and the coil lies between $z=0.12$ m and $z=0.15$ m; it has a voltage of -100 V. The plasma radius (half-density radius) is 0.036 m, the peak density is 8.632×10^{11} m^{-3}, and the temperature is $T=0.01$ eV. This rather odd shape, characteristic of non-neutral plasmas of large radius, is also displayed in Ref. 2.

II. THREE EQUILIBRIUM TYPES

There are probably many different ways of choosing the density function on the right-hand side of Eq. (1). We choose here to describe three which are of particular interest in theoretical and experimental studies of non-neutral plasmas. We first discuss the case of global thermal equilibrium, as described by O'Neil and Driscoll[4] and by Prasad and O'Neil.[2] We next discuss equilibria for which the midplane radial density profile is chosen, and the corresponding two-dimensional distribution of density and potential is to be found. These equilibria are potentially of interest in calculating the effect of finite-length on the dynamics of plasmas whose properties, assuming infinite length, are known (plasmas with hollow density profiles, for example). Finally, we discuss equilibria for which the radial profile of line density, $\int n(r,z)dz$, is known. These equilibria are of special interest to experimenters for whom the measurement of this profile by means of dumping the plasma onto end rings is a standard diagnostic.

In all three of these cases the nonlinear Eq. (1) is solved iteratively, making it possible to make changes in the form of the function $f(r,\phi)$ during calculation to obtain equilibria with various desired properties. Each of these cases and the adjustments to $f(r,\phi)$ peculiar to each one will now be discussed in turn.

A. Thermal equilibrium

The properties of non-neutral plasmas in global thermal equilibrium have been discussed by O'Neil and Driscoll,[4] by Prasad and O'Neil,[2] and by Peurrung and Fajans.[5] In this case the right-hand side of Eq. (1) takes the form

$$f(r,\phi)=A\exp\left(-\frac{q}{kT}\phi(r,z)+\frac{m}{2kT}r^2\omega(\omega+\omega_c)\right),\tag{5}$$

where m is the particle mass, ω_c is the cyclotron frequency, including the sign of the charge, and ω is related to the canonical angular momentum of the system, as discussed by Prasad and O'Neil.[2] Following O'Neil and Driscoll, we rewrite this function in the form

$$f(r,\phi)=-\frac{qn_0}{\epsilon_0}\exp\left(-\frac{q}{kT}(\phi-\phi_{00})-\alpha r^2\right),\tag{6}$$

where ϕ_{00} is the potential at the center of the plasma and where α is a constant to be determined. One advantage of this form is that the central density, n_0, may simply be specified at the outset. A second advantage is that we can choose the radius of the plasma in the midplane r_p (defined to be the radius at which the density has fallen to half of its central value) by iteratively solving Eq. (1) with α readjusted at each step of the iteration according to the formula

$$\alpha=-\frac{q}{kTr_p^2}(\phi(r_p,0)-\phi(0,0))+\frac{\ln 2}{r_p^2}.\tag{7}$$

B. Midplane radial profile

It is often desirable to find an equilibrium with a specified midplane radial density profile. This may be accomplished by using for the right-hand side function

$$f(r,\phi)=-\frac{qn_0}{\epsilon_0}h(r)\exp\left(-\frac{q}{kT}(\phi(r,z)-\phi(r,0))\right),\tag{8}$$

where $\phi(r,0)$ is the electrostatic potential in the midplane of the equilibrium. The radial profile function $h(r)$ is chosen to have value unity at $r=0$ so that n_0 is the central density. We find that equilibria of this kind are the easiest to calculate numerically.

C. Line density profile

When attempting to match an equilibrium calculation to data obtained from dumping a non-neutral plasma onto charge-collection rings, it is desirable to find an equilibrium which matches a specified radial profile of the line density,

$$g(r)=\int_0^b n(r,z)dz.\tag{9}$$

This may be accomplished by using the same form for $f(r,\phi)$ as used in the midplane radial profile case [see Eq. (8)] but with the radial profile function at the nth iteration level given by

$$n_0h^n(r)=\frac{g(r)}{\int_0^b\exp[-(q/kT)(\phi^n(r,z)-\phi^n(r,0))]dz}.\tag{10}$$

This calculation does not perform as well as the thermal equilibrium and midplane radial profile calculations, taking about twice as many iterations to converge. This is presumably because of the added complication of folding the line density into the iteration.

III. BICUBIC SPLINES WITH UNDERRELAXATION

We now discuss the solution of Eq. (1) using bicubic splines. Although more difficult to program than finite-

differences on a grid, this method provides high accuracy with a relatively small number of splines in the r and z directions, and it also provides a high-order interpolation scheme for representing the potential and density at arbitrary points in (r,z). This calculation splits naturally into two parts: first, the operator on the left-hand side of Eq. (1) must be represented in such a way that it can be inverted, and second, an algorithm must be designed to cope with the nonlinear right-hand side. We will discuss the representation of the operator first.

A. Spline representation of ∇^2

For the spline approximation to the potential field $\phi(r,z)$ we use a rectangular subdivision of the region of interest, partitioning the axial interval into n_z elements and the radial interval into n_r elements. We then use a tensor product spline representation of the potential:

$$\phi(r,z) = \sum_{i,j} c_{ij}\psi_i(r)\psi_j(z), \qquad (11)$$

where the functions $\psi_i(r),\psi_j(z)$ are cubic B-splines, $B_k(\cdot)$, with compact support or linear combinations of them at the boundaries. These spline functions are normalized and computed in recursive fashion as described in Schumaker.[6] The boundary conditions are handled by putting appropriate conditions on the coefficients of splines near the boundaries in the usual way. The expansion coefficients c_{ij} are determined by using a Galerkin method: substitute Eq. (11) into Eq. (1), multiply the resulting equation by $\psi_l(r)\psi_m(z)$, for splines in the interior, and integrate over the region of interest. After an integration by parts, an equation of the form

$$\mathbf{A}\cdot\mathbf{c}=\mathbf{b} \qquad (12)$$

results where the elements of the matrix $\mathbf{A}$ are integrals over spline functions. These integrals can be done just once and the matrix $\mathbf{A}$ can be put in lower-triangular-upper-triangular (LU) form, making efficient iteration possible. Note that the overlap integrals used in this method make the matrix $\mathbf{A}$ a banded matrix.

The banded coefficient matrix in Eq. (12) requires $8(n_z+1)(n_r+2)(6n_r+19)$ bytes of storage, and at first glance it would appear that these wide bands would make this method less desirable than a simple finite-difference method requiring a smaller operator. This difficulty is made less severe by the higher accuracy of the splines, which makes it possible to get high accuracy with a relatively small number of knot points. It is true, however, that if storage limitations are an issue, then it is better to use a simple finite-difference scheme like the simultaneous overrelaxation algorithm discussed in Sec. IV.

B. Picard iteration with underrelaxation

We will now discuss how the spline-representation of the operator discussed above can be used to solve Eq. (1) by using successive substitution (often called Picard iteration) with underrelaxation. This scheme is given by

$$\nabla^2\phi^* = f(r,\phi^n), \qquad (13)$$

$$\phi^{n+1} = (1-\epsilon)\phi^n + \epsilon\phi^*, \qquad (14)$$

where ϕ^* is to be found by inverting the spline representation of ∇^2, as discussed above, and where ϵ is chosen to be small enough that the algorithm converges. To make an estimate of how small ϵ must be, it is necessary to do the standard linear eigenvalue analysis of the iterated map given by Eqs. (13) and (14). This analysis is facilitated by replacing the rather complicated function $df/d\phi$ by a simple estimate of its magnitude,

$$\frac{df}{d\phi} \sim \frac{q^2 n_0}{\epsilon_0 k T} = \frac{1}{\lambda_{\mathrm{D}}^2}, \qquad (15)$$

where λ_{D} is the Debye length corresponding to the maximum density in the equilibrium. Making this approximation and computing the eigenvalues of ∇^2 in the cylindrical computation region gives the following estimate for the eigenvalue which makes simple successive substitution into Eq. (13) diverge:

$$\lambda_c = \frac{-1}{[(\pi/2b)^2 + (2.4048/a)^2]\lambda_{\mathrm{D}}^2}. \qquad (16)$$

If the particles in the equilibrium are to form a plasma, then the Debye length must be small compared to the dimensions of the plasma, making λ_c a large negative number. Underrelaxation [Eq. (14)] simply remaps the eigenvalues according to the formula

$$\lambda_{\mathrm{new}} = 1 - \epsilon + \epsilon\lambda_{\mathrm{old}} \qquad (17)$$

so a small positive ϵ can map λ_c to a value a little bigger than -1. If ϵ is made too small, however, then the small eigenvalues of Eq. (13) will be changed by Eq. (17) to values near $+1$, which gives slow convergence. About the best we can do is to make the absolute magnitudes of the eigenvalues corresponding to λ_c and zero be the same, giving

$$\epsilon \approx \frac{2}{2-\lambda_c}. \qquad (18)$$

Numerical experiments confirm that this is indeed a good rough estimate of how small ϵ must be to obtain convergence. Naturally it is desirable to find the value of ϵ which gives the best convergence, and in practice we often find that we get better results with a value of ϵ which is higher by 50%, or so, than the value given by Eq. (18).

As discussed in Sec. II, there are often other quantities besides ϕ which must in included in the iteration, i.e., the constant α which determines the plasma radius for global thermal equilibrium and the function $h(r)$ which is used in the calculation of line-density equilibria. These quantities are simply updated appropriately after each direct solve.

This algorithm works quite well, giving accurate results for a surprisingly small number of splines. We find that to compute an equilibrium to 1% accuracy it is necessary to have the spline knot points spaced no more than about two Debye lengths apart. This is to be contrasted with the finite-difference algorithm, discussed in the next section, which requires about two grid points per Debye length for comparable accuracy.

IV. FINITE-DIFFERENCES WITH NEWTON SOR

We now discuss the solution of Eq. (1) using the finite-difference approximation and simultaneous overrelaxation with Newton's method (Newton SOR). We have chosen this method because it is simple, uses very little memory, and is adequate for equilibrium calculations. We would not recommend this stodgy method for use in a simulation, for example, where it would be necessary to solve for ϕ thousands of times. In such a case something more sophisticated, like a direct matrix method, a multigrid method, etc., would be called for. But in an equilibrium calculation with a severe nonlinearity, like the exponential one which occurs in Eq. (1), more powerful methods must usually be slowed down (by underrelaxing, for instance) to the point where they may be no faster than good old SOR. In addition, the simplicity of SOR makes it relatively easy to respond to the novel changes of geometry invented by creative experimenters. With the addition of Newton's method to efficiently handle the nonlinearity, SOR becomes a very simple and powerful way to solve these nonlinear equations.

This method begins by subdividing the computation region into rectangular cells with n_r divisions in the radial direction and n_z divisions in the axial direction. The equilibrium potential, ϕ, is represented by its value in the center of each cell. In the discussion that follows, ϕ_{ij} is the value of ϕ in the cell with radial index i and axial index j whose center is at (r_i, z_j). A straightforward implementation of SOR, as described in Ref. 7, to Eq. (1) gives

$$\phi_{ij}^{n+1} = \frac{\omega}{2(1/\Delta r^2 + 1/\Delta z^2)}$$
$$\times \left(\frac{[(1+\Delta r/2r_i)\phi_{i+1,j}^n + (1-\Delta r/2r_i)\phi_{i-1,j}^{n+1}]}{\Delta r^2} \right.$$
$$\left. + \frac{[\phi_{i,j+1}^n + \phi_{i,j-1}^{n+1}]}{\Delta z^2} - f(r, \phi_{ij}^n) \right) + (1-\omega)\phi_{ij}^n$$

(19)

where $\Delta r = a/n_r$, where $\Delta z = b/n_z$, and where ω is an acceleration factor with a value between 1 and 2. In practice we find that a good estimate for the best value of ω is the same value given in Ref. 7 for Poisson's equation with Dirichlet boundary conditions on a rectangle:

$$\omega = \frac{2}{1 + \sqrt{1 - \rho^2}},$$

(20)

$$\rho = \frac{\Delta z^2 \cos(\pi/n_r) + \Delta r^2 \cos(\pi/n_z)}{\Delta z^2 + \Delta r^2}.$$

(21)

Note that the mix of iteration levels on the right-hand side of Eq. (19) is simply the result of using updated values of ϕ as soon as they become available. Here we have assumed that the algorithm starts in the cell in the lower left-hand corner of Fig. 1 and proceeds radially first. (The red-black, or odd–even, ordering recommended in Ref. 7 for SOR does not improve the convergence of the nonlinear problems discussed in this paper.)

This algorithm can be improved, for nonlinear problems like the ones discussed here, by trying to put $f(r, \phi)$ at the $n+1$ iteration level, as follows

$$f(r, \phi^{n+1}) = f(r, \phi^n + (\phi^{n+1} - \phi^n))$$
$$\approx f(r, \phi^n) + \frac{\partial f}{\partial \phi^n}(\phi^{n+1} - \phi^n).$$

(22)

The term containing ϕ^{n+1} is moved to the left-hand side of the iteration equation to obtain the Newton-SOR algorithm:

$$\phi_{ij}^{n+1} = \frac{\omega}{2(1/\Delta r^2 + 1/\Delta z^2) + \partial f/\partial \phi_{ij}^n}$$
$$\times \left(\frac{[(1+\Delta r/2r_i)\phi_{i+1,j}^n + (1-\Delta r/2r_i)\phi_{i-1,j}^{n+1}]}{\Delta r^2} \right.$$
$$\left. + \frac{[\phi_{i,j+1}^n + \phi_{i,j-1}^n]}{\Delta z^2} - f(r, \phi_{ij}^n) + \frac{\partial f}{\partial \phi_{ij}^n} \phi_{ij}^n \right)$$
$$+ (1-\omega)\phi_{ij}^n.$$

(23)

Changing the algorithm in this way improves the convergence markedly, and is, in fact, Newton's method, as discussed in Ref. 8. In practice, however, the algorithm does not exhibit the usual sensitivity to initial conditions expected of Newton's method, perhaps because SOR propagates information so slowly across the grid.

As discussed in Sec. II, there are often other quantities besides ϕ which must be included in the iteration, i.e., the constant α which determines the plasma radius for global thermal equilibrium and the function $h(r)$ which is used in the calculation of line-density equilibria. These quantities are simply updated as described in Sec. II after each Newton-SOR pass over the entire grid.

We find that this algorithm is surprisingly robust, finding equilibria successfully even if the Debye length is small or if the density is high enough to push the plasma nearly past the confining coil. We find that to obtain 1% accuracy it is necessary to have two grid points per Debye length in the r and z directions, four times the resolution (in each direction) required by the bicubic spline algorithm. Newton SOR has modest memory requirements, is simple to use, and is easy to modify. Its simplicity has allowed us to mold it into a rather versatile tool, allowing a wide range of choices for boundary conditions and even the presence of arbitrarily shaped conductors inside the cylinder. This code is available upon request.

In the next section we describe tests we have made with both the spline and finite-difference algorithms, comparing them with each other and with known properties of the most-studied non-neutral plasma equilibrium: global thermal equilibrium.

V. COMPARISONS WITH GLOBAL THERMAL EQUILIBRIUM

In this section we compare the results of both the spline algorithm and the finite-difference algorithm with the known properties of global thermal equilibria. We also

4270   Phys. Fluids B, Vol. 5, No. 12, December 1993

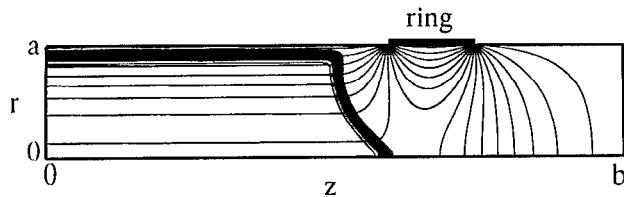Spencer, Rasband, and Vanfleet   4270

ring

FIG. 2. The density and potential contours of a low temperature thermal equilibrium non-neutral plasma with large radius and a weak confining voltage is displayed. The parameters are the same as in Fig. 1 except that the voltage on the ring is only -12 V. This plasma is ill confined, and hence has a neck that extends into the confining cylinder, as discussed in Ref. 5.

present a new characterization of these equilibria which is especially useful in testing the accuracy of numerical calculations.

As a first example, consider Fig. 1. This displays the density contours of a large-radius thermal equilibrium computed using the spline algorithm with $nr=25$ and $nz=125$. The temperature is 0.01 eV and the central density is $n_0=8.632\times10^{11}$ m^{-3}; this density value is chosen to make the radius of the conducting wall be 50 Debye lengths (using the central density). The rather odd shape shown in this figure is the same as that shown in Ref. 2. An equilibrium with such a small Debye length is difficult to calculate, yet this equilibrium required less than an hour on an RS/6000 workstation.

As a second example, consider Fig. 2. In addition to the difficulties of Fig. 1, we have made the plasma ill-confined, as discussed by Peurrung and Fajans.[5] Note that the center of the plasma has bulged toward the weak potential hill that just barely holds it in. This finite-difference calculation is less accurate than that in Fig. 1 since it uses finite differences and only a 50×250 grid was used, but the overall plasma shape is still quite accurate. This calculation also took less than an hour on an RS/6000.

To examine the accuracy of these computed equilibria more closely, it is helpful to have detailed information about the shape of the density fall-off region of global thermal equilibria. Such information can, of course, be obtained by numerically integrating the appropriate differential equation, as discussed in Ref. 4, but an analytic way of characterizing this region would be more useful. To obtain such a result we begin with the equilibrium equations given by O'Neil and Driscoll.[4] Translated into our notation [see our Eq. (6)] their quantity ψ is given by

$$\psi=-\frac{q}{kT}(\phi-\phi_{oo})-\alpha r^2 \qquad (24)$$

and the differential equation, appropriate for describing the radial distribution of density in an infinitely long non-neutral plasma in global thermal equilibrium, is

$$\psi''+\frac{1}{\rho}\psi'=e^{\psi}-1-\gamma, \qquad (25)$$

where $\rho=r/\lambda_{\mathrm{D}}$, where the prime denotes a derivative with

respect to ρ, and where $\gamma=4\alpha\lambda_{\mathrm{D}}^2-1$. When the plasma radius is large compared to the Debye length O'Neil and Driscoll show that

$$\gamma\approx\ln 2\sqrt{2\pi\rho_p}e^{-\rho_p}, \qquad (26)$$

with $\rho_p=r_p/\lambda_{\mathrm{D}}$.

We characterize the density fall-off region by computing the gradient scale length of the density, $n\propto\exp\psi$, at the half-density point,

$$\frac{1}{\rho_s}=\frac{dn/d\rho}{n}=\psi'(\rho_p), \qquad (27)$$

where this scale length is in units of the Debye length. We begin by ignoring γ and the $1/\rho$ term in Eq. (25), since $\rho_p\gg1$. We then multiply Eq. (25) by ψ' and integrate to obtain

$$\psi'\approx\sqrt{2(\exp(\psi)-1-\psi)}. \qquad (28)$$

Evaluating this at the half-density point, $\psi=-\ln 2$, gives

$$\rho_s\approx\frac{1}{\sqrt{2\ln 2-1}}, \qquad (29)$$

which is a good approximation for the radial gradient scale length if $r_p\gg\lambda_{\mathrm{D}}$. Because we have dropped the $1/\rho$ term in Eq. (25), the differential equation in ρ is the same as the axial differential equation in z/λ_{D}, making this formula an even better approximation for the axial gradient scale length at the end of the plasma, provided that the radius of curvature of the plasma at the end is much greater than λ_{D}. (It would not be a good approximation at the tip of the equilibrium shown in Fig. 2, for example; these issues are discussed by Peurrung and Fajans.[5]) We may obtain a correction of order $1/\rho_p$ by keeping the term containing $1/\rho$ in Eq. (25), but replacing $1/\rho$ by $1/\rho_p$ and by replacing ψ' by the expression in Eq. (28) to obtain

$$\psi''=e^{\psi}-1+\frac{\sqrt{2}}{\rho_p}\sqrt{\exp(\psi)-1-\psi}, \qquad (30)$$

where we have ignored γ because it is much smaller than $1/\rho_p$. We again multiply by ψ' and integrate from the half-density point where $\psi=-\ln 2$ to the top of the density profile where $\psi=0$:

$$\frac{1}{\rho_s^2}\approx2\ln 2-1+\frac{\sqrt{2}}{\rho_p}\int_0^{-\ln 2}\sqrt{\exp(\psi)-1-\psi}\,d\psi. \qquad (31)$$

Numerically performing the definite integral and rearranging gives, to first order in $1/\rho_p$,

$$\rho_s\approx\frac{1}{\sqrt{2\ln 2-1}}\left(1+\frac{0.5778}{\rho_p}\right). \qquad (32)$$

The difference between this formula and Eq. (29) gives a good estimate of how self-similar the density fall-off will be around the edge of a plasma in global thermal equilibrium. For the case discussed by Prasad and O'Neil[2] $\rho_p=10$ which means that the density profiles discussed in their

paper should only be self-similar to within about 5%; this estimate is consistent with the variation in ψ' displayed in their Fig. 4.

We have made extensive tests of this formula against numerical solutions of Eq. (25) and we find that it is accurate to better than 1% for $\rho_p > 10$. We have also tested both the spline algorithm and the finite-difference algorithm against these formulas and find excellent agreement, if enough splines or grid points are taken. We find that to obtain an accuracy of 1% in the computation of the gradient scale length it is necessary that the splines be spaced not more than about two Debye lengths apart and that the grid points in the finite difference calculation must be no larger than $\lambda_D/2$. This is a rather rigorous test since it depends on the gradient of the potential; more global quantities like plasma potential, total number of particles, and plasma shape are computed even more accurately by both codes. If one is only interested in such quantities, the restrictions on spline separation and grid spacing may be further relaxed.

Finally, we have compared the speed of the finite-difference and spline algorithms by comparing the times required by each code to achieve the same accuracy on the same machine. The number of grid points in the radial and axial directions in the finite-difference code was four times the corresponding number of splines to achieve comparable spatial accuracy as discussed above. We found that the spline code was about 50% faster than the finite-difference code.

VI. CONCLUSION

We have found and extensively tested two algorithms for computing three different kinds of non-neutral plasma equilibria: (i) plasmas which are in thermal equilibrium, (ii) plasmas whose midplane radial density profiles are specified, and (iii) plasmas whose line density profiles, $\int_0^b n(r,z)dz$, are specified. For high-accuracy calculations we prefer to use Picard iteration and splines with underrelaxation, provided that many megabytes of computer memory are available. If large amounts of memory are unavailable, or if high accuracy is not as important as having a relatively simple algorithm which gives good results if a fine enough grid is used, then we prefer SOR with finite-differences and Newton's method. Finally, we have obtained a formula for the gradient scale length at the half-density point, including a first-order correction in the ratio of the Debye length to the plasma radius, which makes it relatively easy to test the accuracy of equilibrium calculations.

[1] J. H. Malmberg and J. S. DeGrassie, Phys. Rev. Lett. **35**, 577 (1975).
[2] S. A. Prasad and T. M. O'Neil, Phys. Fluids **22**, 278 (1979).
[3] G. Bateman, *MHD Instabilities* (MIT Press, Cambridge, MA, 1978), Chap. 4.
[4] T. M. O'Neil and C. F. Driscoll, Phys. Fluids **22**, 266 (1979).
[5] A. J. Peurrung and J. Fajans, Phys. Fluids B **2**, 693 (1990).
[6] L. Schumaker, *Spline Functions* (Wiley, New York, 1981).
[7] W. H. Press, B. P. Flannery, S. A. Teukolsky, and W. T. Vetterling, *Numerical Recipes* (Cambridge University Press, Cambridge, 1986), Chap. 17.
[8] R. E. White, *An Introduction to the Finite Element Method with Application to Nonlinear Problems* (Wiley, New York, 1985), p. 208.